Accepted Manuscript

Discovery of 3(*S*)-thiomethyl pyrrolidine ERK inhibitors for oncology

Sobhana Babu Boga, Abdul-Basit Alhassan, Alan B. Cooper, Ronald Doll, Neng-Yang Shih, Gerald Shipps, Yongqi Deng, Hugh Zhu, Yang Nan, Robert Sun, Liang Zhu, Jagdish Desai, Mehul Patel, Kiran Muppalla, Xiaolei Gao, James Wang, Xin Yao, Joseph Kelly, Subrahmanyam Gudipati, Sunil Paliwal, Hon-Chung Tsui, Tong Wang, Bradley Sherborne, Li Xiao, Alan Hruza, Alexei Buevich, Li-Kang Zhang, David Hesk, Ahmed A. Samatar, Donna Carr, Brian Long, Stuart Black, Priya Dayananth, William Windsor, Paul Kirschmeier, Robert Bishop

PII: S0960-894X(18)30373-1
DOI: https://doi.org/10.1016/j.bmcl.2018.04.063
Reference: BMCL 25810

To appear in: *Bioorganic & Medicinal Chemistry Letters*

Received Date: 22 February 2018
Revised Date: 10 April 2018
Accepted Date: 25 April 2018

Please cite this article as: Boga, S.B., Alhassan, A-B., Cooper, A.B., Doll, R., Shih, N-Y., Shipps, G., Deng, Y., Zhu, H., Nan, Y., Sun, R., Zhu, L., Desai, J., Patel, M., Muppalla, K., Gao, X., Wang, J., Yao, X., Kelly, J., Gudipati, S., Paliwal, S., Tsui, H-C., Wang, T., Sherborne, B., Xiao, L., Hruza, A., Buevich, A., Zhang, L-K., Hesk, D., Samatar, A.A., Carr, D., Long, B., Black, S., Dayananth, P., Windsor, W., Kirschmeier, P., Bishop, R., Discovery of 3(*S*)-thiomethyl pyrrolidine ERK inhibitors for oncology, *Bioorganic & Medicinal Chemistry Letters* (2018), doi: https://doi.org/10.1016/j.bmcl.2018.04.063

ELSEVIER

Bioorganic & Medicinal Chemistry Letters
journal homepage: www.elsevier.com

Discovery of 3(*S*)-thiomethyl pyrrolidine ERK inhibitors for oncology[#]

Sobhana Babu Boga[a,*], Abdul-Basit Alhassan[a], Alan B. Cooper[a], Ronald Doll[a], Neng-Yang Shih[a], Gerald Shipps[b], Yongqi Deng[b], Hugh Zhu[a], Yang Nan[b], Robert Sun[a], Liang Zhu[b], Jagdish Desai[a], Mehul Patel[b], Kiran Muppalla[b], Xiaolei Gao[a], James Wang[a], Xin Yao[a], Joseph Kelly[a], Subrahmanyam Gudipati[a], Sunil Paliwal[a], Hon-Chung Tsui[a], Tong Wang[b], Bradley Sherborne[a] Li Xiao[a], Alan Hruza[a], Alexei Buevich[a], Li-Kang Zhang[a], David Hesk[a], Ahmed A. Samatar[a], Donna Carr[a], Brian Long[a], Stuart Black[a], Priya Dayananth[a], William Windsor[a], Paul Kirschmeier[a], Robert Bishop[a]

[a] *Discovery Chemistry, Merck & Co., Inc.,2015 Galloping Hill Rd, Kenilworth, NJ 07033, United States*
[b] *Discovery Chemistry, Merck & Co., Inc., 33 Avenue Louis Pasteur, Boston, MA 02115, United States*

[#]*Dedicated to Professor Dale L. Boger, Professor The Scripps Research Institute, San Diego, CA, USA on the occasion of his 65th birthday*

ARTICLE INFO

Article history:
Received
Revised
Accepted
Available online

Keywords:
ERK inhibitor
ATP competitive
MAP kinases
Kinase selectivity
Oncology

ABSTRACT

Compound **5**(SCH772984) was identified as a potent inhibitor of ERK1/2 with excellent selectivity against a panel of kinases (0/231 kinases tested @ 100 nM) and good cell proliferation activity, but suffered from poor PK (rat AUC PK @10 mpk= 0 uM.h; F %= 0) which precluded further development. In an effort to identify novel ERK inhibitors with improved PK properties with respect to **5**, a systematic exploration of sterics and composition at the 3-position of the pyrrolidine led to the discovery of a novel 3(*S*)-thiomethyl pyrrolidine analog **28** with vastly improved PK (rat AUC PK @10 mpk= 26 uM.h; F % = 70).

Aberrant and hyper activation of the RAS/RAF/MEK/ERK signaling pathway, a member of the MAPK kinase pathway, plays a central role in the underlying proliferation mechanisms of several human tumor subtypes. ERK is the downstream target of the MAPK kinase pathway and is constitutively activated in many tumor cells (Melanoma: 60% BRAF mutant; 15-20% NRAS, Colon: 50% KRAS mutant, 15% BRAF, Pancreatic: 90% KRAS, NSCLC: 30% KRAS).[1] ERK inhibition selectively induces many cellular events including cell differentiation, cell proliferation and apoptosis.[2] Of late, several highly optimized ERK inhibitors such as the pyrrole **1** by Vertex/Biomed Valley Discoveries,[3] the pyridone **2** by Genentech[4], fused pyrrolo-diazepanone **3** by Novartis[5] and most recently, the irreversible acrylate inhibitor **4** by Astrazeneca[6] have been reported (Figure 1).

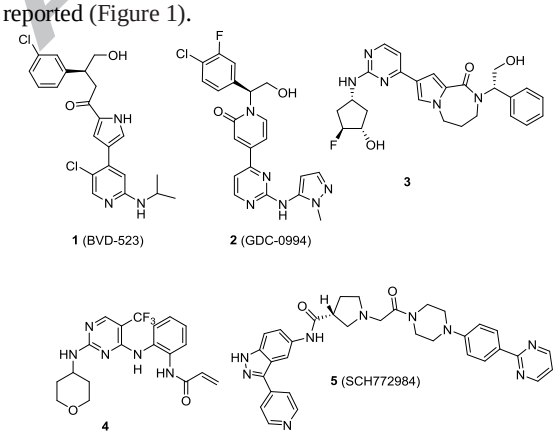

Figure 1. Representative structures of ERK inhibitors **1**-**5**.

An excellent review[7] by Samatar and Poulikakos describes the discovery and development of various RAS-ERK inhibitors that are being studied at various phases in both clinical and pre-clinical development. The seminal work by these groups has led to the development of more effective therapies for patients with tumors dependent on the ERK signaling pathway. The goal of our research effort was to overcome RAS-ERK resistance believed to be tied to down field effectors in the MAPK pathway. Designing potent and selective RAS-ERK inhibitors that could mediate drug resistance is a daunting challenge that has been a major focus for both academia and the pharmaceutical industry.[8] We reported[9] the discovery of a highly potent, kinase selective ERK1/2 inhibitor **5** (SCH772984) that displayed unique dual mechanism of action (inhibits both phosphorylation of ERK and RSK) and demonstrated *anti*-tumor efficacy in both the BRAF/RAS mutant cell line xenograft models (Figure 1).

Compound **5** is a potent ERK inhibitor (ERK2 IC_{50}= 1 nM), exhibiting high kinase selectivity (0/231 kinases tested @ 100 nM), which was derived from an initial high throughput screening hit **6**(ERK2 IC_{50}=18.6 μM) (Figure 2). Compound **6** was obtained through an in-house neomorph small molecule library which was screened against the unphosphorylated (in-active) form of the target protein ERK2 utilizing an automated ligand identification system (ALIS). Subsequent SAR following hit validation from **6** afforded compound **7** (ERK2 IC_{50}=2.7 μM).[10] Introduction of the indazole pharmacophore provided enhanced potency and selectivity giving rise to compound **5**; however, compound **5** suffered from both poor absorption and bioavailability in rat, as seen in the plasma drug concentration measured by area under the concentration-time curve

(AUC) (Rat AUC @ 10 mpk=0 nM.h; F %= 0), that precluded this target for further development. Based upon our interest in developing an oral ERK compound for *in-vivo* biological studies, we chose to further explore the SAR of this novel class of ERK inhibitors. Herein we report our research efforts toward this aim (Figure 2).

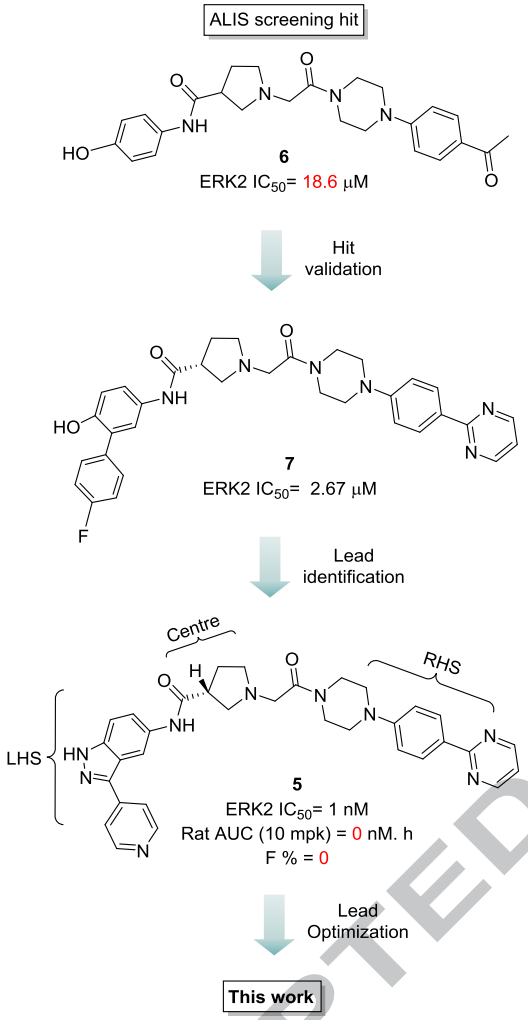

Figure 2. Hit to lead identification of ERK inhibitor **5**(SCH772984).

To enable our structure based drug design (SBDD) effort, we obtained the X-ray crystal structure of **5** bound to ERK2, shown in Figure **4**. The binding mode is similar to other inhibitors in the series and has been extensively discussed previously[10]. Briefly, the two indazole nitrogen atoms of **5** form hydrogen bonds with Asp104 and Met106 at the hinge region of the ERK2 ATP binding site. The pyridine N atom forms an H-bond with Lys112, while the two amide carbonyl O atoms, along with the protonated pyrrolidine N atom, are involved in an H-bond network with gatekeeper Gln103 and catalytic Lys52. In addition, upon binding of **5** to ERK2, the G-loop undergoes a large conformation change which flips the Try34 side-chain and generates a new side pocket for **5** to extend into, thus produces a novel binding conformation where aromatic pi-pi stacking interactions between the pyrrolidine and Tyr34, and the distal phenyl pyrimidine and Tyr62, were observed. This unique binding conformation leads to excellent kinase selectivity for **5** and its analogs.

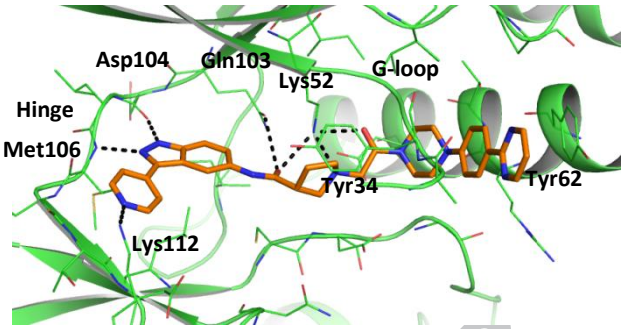

Figure 3. X-ray crystal structure of **5** in the active site of ERK2 with hydrogen bond interactions to the key residues highlighted in dashed lines

Based on the X-ray studies, the pyrrolidine amide linkage is involved in pivotal hydrogen bonding interactions in the active site with the gate keeper residues (Asp165, Gln103 Glu69) of the ERK protein vis-à-vis a water hydrogen bond network (depicted in Figure 3). We began our SAR studies by replacing the unsubstituted pyridine (potentially susceptible to *N*-oxide formation mediated by cytochrome P450 enzymes) at the 3-position of the indazole, which has a key interaction with the lysine 112 residue of ERK, with a *p*-fluoro phenyl group to afford compound **8**. Compound **8** maintained ERK potency ERK2 IC_{50}= 5.5 nM, but did not show any sign of improving pharmacokinetics (PK) in the rat (Rat AUC @ 10 mpk=0 nM.h) Table **1**.

In order to better understand the underlying mechanism for poor bioavailability for this class of compounds, metabolic identification studies with compound **8** were undertaken. Incubation of compound ^{3}H-**8** in cryo-preserved rat and human hepatocytes at 10 µM and 1 µCi/mL for 0, 2 and 4 hours at 37°C followed by metabolite characterization identified the indazole amide linkage as the major metabolic pathway giving rise to metabolites **9** and **10** (Figure-**4**).

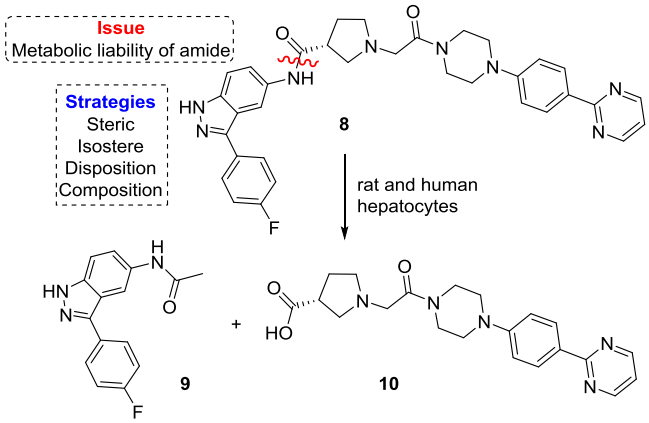

Figure 4. Metabolic pathway and strategies for mitigating the amide bond cleavage liability of **8**

Guided by *in-silico* modeling, an initial chemistry strategy was aimed at structural modifications (*viz*., elimination, disposition, isostere and steric hindrance) around the pyrrolidine amide region in an effort to mitigate this metabolic pathway. We first investigated the simple elimination of the carbonyl group (compound **11**) and disposition of the amide as the *N*-acetyl (compound **12**), both of which caused significant loss in ERK activity compared to compound **8**. Incorporation of a triazole as an amide isostere, (compound **13**) was unfortunately shown to be completely devoid of ERK activity illustrating the significance of the pyrrolidine amide group with respect to ERK inhibition.

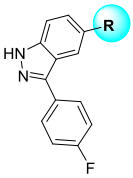

Table 1. Significance of pyrrolidine amide group towards ERK potency

#	R	ERK2 IC_{50} (nM)	Rat AUC @10 mpk (nM.hr)
8	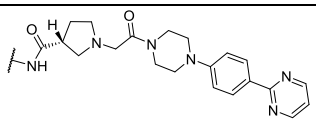	5.5	0
11	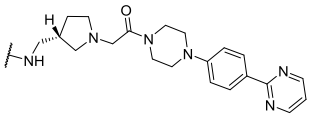	960	ND
12	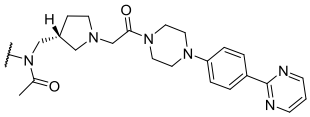	574	ND
13	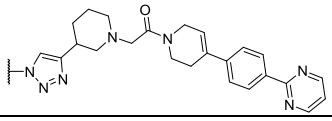	>1000	ND

[ND] Not Determined

We then chose to determine whether electronic and steric interactions could affect amide metabolism and as such provide a path forward for this promising chemo type, lead **5**. A systematic SAR at the 3- position of the pyrrolidine amide (centre core) while keeping the same p-flouro phenyl indazole Left Hand Side (LHS) and in combination with two of the Right Hand Sides (RHS) (R^2= pipirazine **8** and pipiridine-*ene* **14)** was explored as depicted in Table 2. In general smaller substitutions at the 3-position of the pyrrolidine (viz., methyl **15** and fluoro methyl **16)** retained ERK potency but did not show any significant improvement in rat AUC levels. Incorporation of heteroatom polar functionality such as hydroxy methyl **17** and *N*, *N*-dimethyl compound **18** had slightly weaker ERK potency. However, introduction of the 3(*R*)-methoxy moiety, compound **19** resulted in a modest measurable AUC of 352 nM in rat following 10 mpk dose, while retaining ERK potency. Notably, compound **20** (R^2= pipiridine-*ene* RHS) showed a 5 fold improvement in rat PK (AUC=1.8 µM.h) while retaining single digit nanomolar ERK potency. Increasing the length and size of the alkoxy group, such as ethoxy **21**, *iso*propoxy **22** and phenoxy **23,** seemed to be very sensitive and generally not well tolerated leading to loss in ERK potency but/albeit showed some improvement in rat AUC levels. Attempted substitutions of methoxymethyl compounds **24, 25** and ethyl compound **26** resulted in a 5 to 20 fold loss in ERK potency compared to compound **8**.

Further SAR exploration led to the incorporation of a thiomethoxy group at the 3-position of the pyrrolidine to afford compounds **27** and **28**. The 3(*S*)-thiomethoxy pyrrolidine analogs **27** and **28** showed a dramatic 10-14 fold improvement in rat AUC levels at 10 mpk PO dose (AUC=3.6 µM.h for **27**; 26 µM at 10 mpk for **28**) compared to the corresponding 3(*R*)-methoxy pyyrolidine analogs (AUC=0.35 µM.h for 19; AUC=1.8 µM.h for **20**) while retaining single digit nanomolar ERK potency. Although sterically hindered tertiary 3(*S*)-thiomethoxy pyrrolidine compound **28** was stable to aerial oxidation at ambient temperature, the corresponding sulfone methyl analog **29** was detected following chemical oxidation with *m*CPBA[11]. Sulfone methyl compound **29** displayed weaker ERK potency and did not have a significant PK advantage when compared to thiomethyl compound **28**. To capitalize on the observed PK enhancements observed following the substitution of the 3(*S*)-methoxy and 3(*S*)-thiomethoxy groups at the 3-position of the pyrrolidine we chose to explore similar groups in the hope that they might provide further improved PK properties. Attempted ring expansion to morpholine compound **30** and thiomorpholine compound **31** led to a loss of ERK2 potency, potentially disturbing the close interaction with the gate keeper region of the active site of the ERK protein. Interestingly, the opposite enantiomer 3(*R*)-thiomethoxy compound **32**[12] was shown to be completely devoid of ERK potency, highlighting the stereospecific constraints and stringent structural composition requirements for this class of inhibitors to maintain ERK potency.

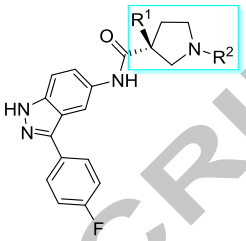

Table 2. Exploration of center core toward ERK activity and PK.

Centre core R^1 =	R^2 = 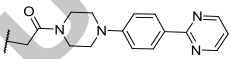 #; ERK2 IC_{50} (nM) / Rat AUC (nM.h)[$]	R^2 = 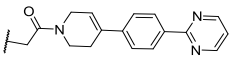 #; ERK2 IC_{50} (nM) / Rat AUC (nM.h)[$]
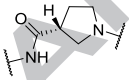	**8**; 5.5/0	**14**; 15.5/ND
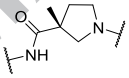	**15**; 24/65	-
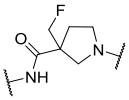	**16**; 5.8/28	-
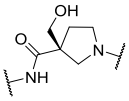	-	**17**; 14/ND
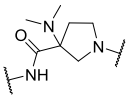	-	**18**; 21/ND
	**19**; 2.1/352	**20**; 4.8/1880
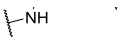	**21;** 9.7/150	-
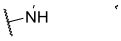	**22**; 90/712	-
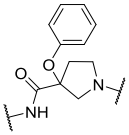	**23**; >3000/938	-
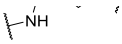	**24;** 25/1216	**25;** 41/ND
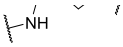	-	**26**; 115/ND

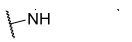	**27**; 5.6/3657	**28**; 7/25914
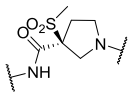	-	**29**; 12/4091
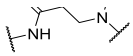	-	**30**; 119/ND
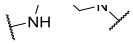	-	**31**; 1311/ND
	-	**32**; >3000/ND

ND Not Determined $ Rapid Rat PK dosed @ 10 mpk

As depicted in Table **2**, 3(*S*)-thiomethoxy pyrrolidine compound **28** emerged as a lead ERK inhibitor with single digit nanomolar potency and an improved PK profile. Further evaluations of compound **28** versus the 3(*S*)-methoxy pyrrolidine compound **20** and the initial proof of concept lead pyrrolidine compound **5** were conducted across various parameters (viz., enzymatic, cellular potency, CYP, hERG, Caco-2 permeability and PK) and are summarized in Table **3**. Compound **28** maintained good ERK enzymatic activity (ERK IC_{50} = 7 nM) and cellular activity in *BRAF/KRAS* mutant wildtype cancer cell lines (HT-29/Caspase IC_{50} (nM) = 118/80 nM) compared to compounds **20** and **5**. Interestingly, swapping the methoxy to a thiomethoxy group reduced hERG inhibitory activity (hERG %I@1.5/5 mg/ml = 8/21) and human/dog hepatocyte clearance (Hu & Dog hep. CL mL/min/M = 18 & 7), but CYP 3A4 activation still needed to be addressed. The 3(*S*)-thiomethoxy pyrrolidine compound **28** was selected for full *in vivo* PK evaluation in both and rat at 10 mpk PO; 3 mpk IV and in dog at 10 mpk PO; 2 mpk IV, 2mpk IPT (via portal vein infusion). Compound **28** displayed excellent pharmacokinetic profiles with total clearance of 8.4 mL/min/kg, $t_{½}$ of 2.5 h, with 70% bioavailability in the rat and a total clearance of 7.6 mL/min/kg, $t_{½}$ of 2 h, and 75% bioavailability in the dog (Figure 5).

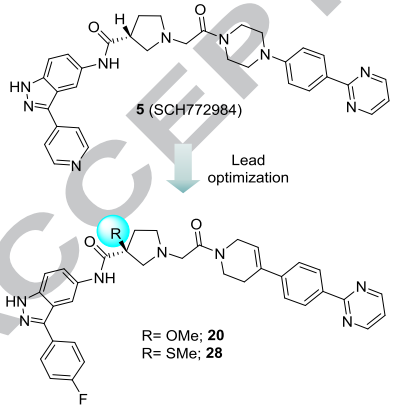

Table 3. Comparison of analogs **5**, **20** and **28** toward overall ERK profile.

Parameter (units)	**5** R = H	**20** R = OMe	**28** R = SMe
ERK2 IC_{50} (nM)	1	4.8	7
HT-29/Caspase IC_{50} (nM)	59/96	88/79	118/80
CYP 3A4 (co/pre) (mM)	7.8/5.7	31/2.2	>30/2
hERG Rb (%I) @1.5/5 mg/ml	12/3	56/70	8/21
Hu & Dog hep. CL (mL/min/M)	ND	36/33	18/7
10^6Caco II (P_{app}/cm.S^{-1})	4		60
Rat AUC @ 10 mpk (nM.hr.)	0	1880	25914
Clp (mL/min/kg)	ND	ND	8.4
t½ (h)	ND	ND	2.5
Mean residence time (hr.)	ND	ND	2.5
Bioavailability F %	0	ND	70
Dog AUC @ 10 mpk (nM.hr.)	ND	4528	17200
Clp (mL/min/kg)	ND	ND	7.6
t½ (h)	ND	ND	2.0
Mean residence time (hr.)	ND	ND	5.1
F %	ND	ND	75

ND Not Determined

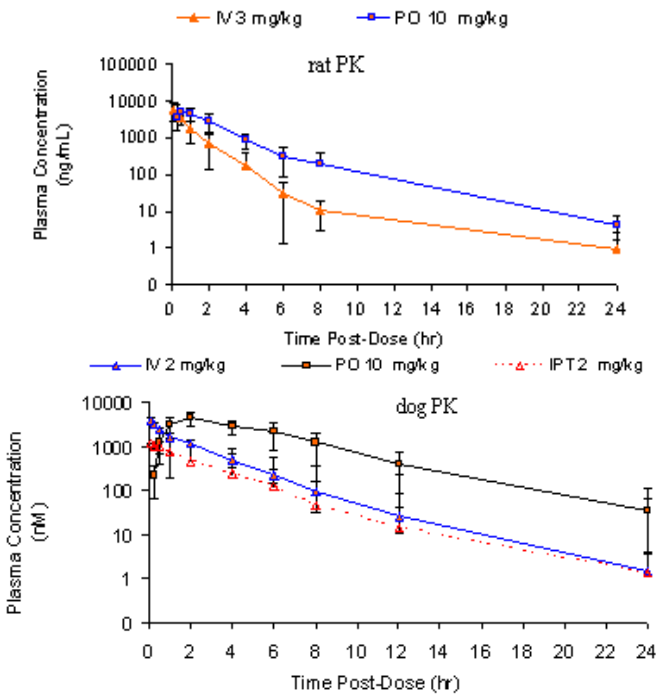

Figure 5. Rat and dog Plasma concentration (Mean ± SD) of compound **28**

We hypothesized that the observed dramatic enhancement of PK for the 3(*S*)-thiomethoxy pyrrolidine ERK inhibitor **28** over compounds **5** and **20** could be due to the combination of both steric hindrance and electronic effects. We envisioned that the thiomethyl group could participate in a strong coordination with zinc in the metalloprotease active site[13], thereby shifting the equilibrium more towards intermediate **34**, reducing the formation of the tetrahedral intermediate **33**, resulting in minimized potential for amide hydrolysis and thus mitigating the amide metabolic liability (Figure **6**). To the best of our knowledge, this is first reported example of an improvement in PK profile resulting from the substitution of a sulfur based group (e.g., thiomethyl) adjacent or in close proximity to an amide functional group.

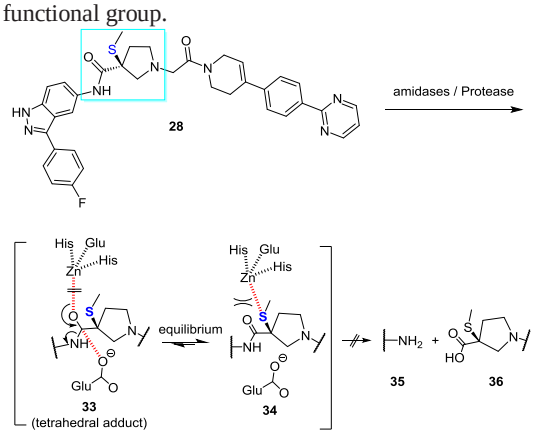

Figure 6. Plausible rationale for the PK enhancements of compound **28**

To understand how 3(*S*)-thiomethoxy group interacts with ERK2, the X-ray structure of ERK2/**27** was determined (Figure **7**, PDB:6CPW). Not surprising, **27** showed a similar binding mode as **5**. The 3(*S*)-thiomethoxy group points into the binding region where Asn152, Leu154, Cys164, and Asp165 serve as the floor, G-loop as the

ceiling, making hydrophobic contacts with Asn152, Cys164, and Try34.

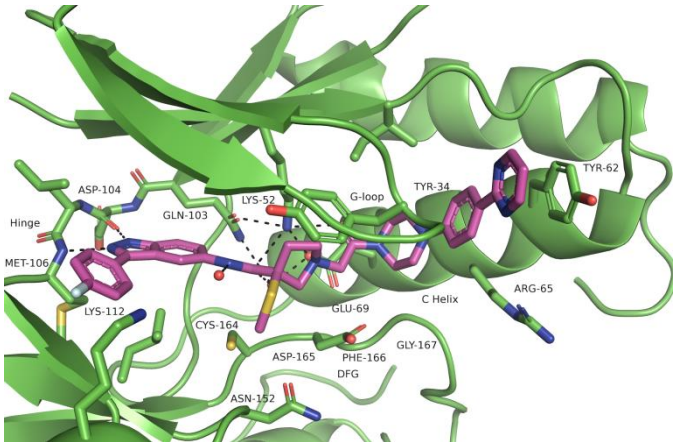

Figure 7. X-ray crystal structure of **27**(PDB:6CPW) in the active site of ERK2 with hydrogen bond interactions to the key residues highlighted in dashed lines.

Since **28** is a close analog of **27**, we expected a similar binding mode of **28** in ERK2 as **27**. A structural model[14] of ERK2/**28** (Figure **8**), constructed using the X-ray structure of ERK2/**27**, displayed the binding conformation of 3(*S*)-thiomethoxy that allows **28** to retain strong binding to ERK2, while offers improved PK profile.

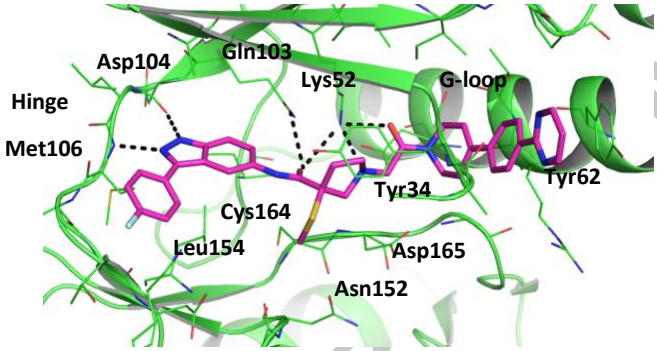

Figure 8. A structural model of **28** in the active site of ERK2. It displays a similar binding mode of **5**, while it's 3(*S*)-thiomethoxy group points towards the binding region defined by residues Asn152 and Cys164.

Synthesis of these ERK inhibitors relied upon on a convergent approach utilizing three fragments *viz*., substituted indazole (LHS), piperidine-*ene* synthon (RHS), and 3(*S*)-thiomethyl pyrrolidine centre core as depicted for compound **28** in Scheme 1. Commercial 3-nitro indazole **37** was brominated followed by Boc protection to afford compound **38** in good yield. Suzuki coupling of **38** with *p*-fluoro phenyl boronic acid followed by hydrogenation using Pd/C generated the LHS **39** in overall good yield. Suzuki coupling of Boc-protected piperidine-*ene* boronic acid **41** with pyrimidine compound **40** afforded **42** in good yield. Deprotection under acidic conditions followed by chloroacetylation generated the RHS **43** in good yield. Novel achiral 3-thiomethoxy pyrrolidine **49** was prepared based on our previously reported synthetic methodolgy[15] involving two synthetic approaches viable for scale-up. Acid catalyzed [3+2] cycloaddition between acrylate **44** and azomethine ylide precursor **45** and thiomethylation of **47** with dimethyl disulfide/LDA at −78°C followed by deprotection gave the 3-thiomethyl Pyrrolidine **48** in moderated yield. Chiral resolution of **49** by crystallization with L-tartaric acid in MeOH led to the synthesis of novel center core 3(*S*)-thiomethyl pyrrolidine **50** in >99% purity.[16] Boc protection and hydrolysis of methyl ester 3(*S*)-thiomethyl pyrrolidine **50** followed by HATU coupling with indazole **43** led to the assembly of fragment **51** in good yield. Global deprotection of **51** using TFA and alkylation of RHS fragment **50** afforded the 3(*S*)-thiomethoxy pyrrolidine ERK inhibitor **28**[17] in good yield.

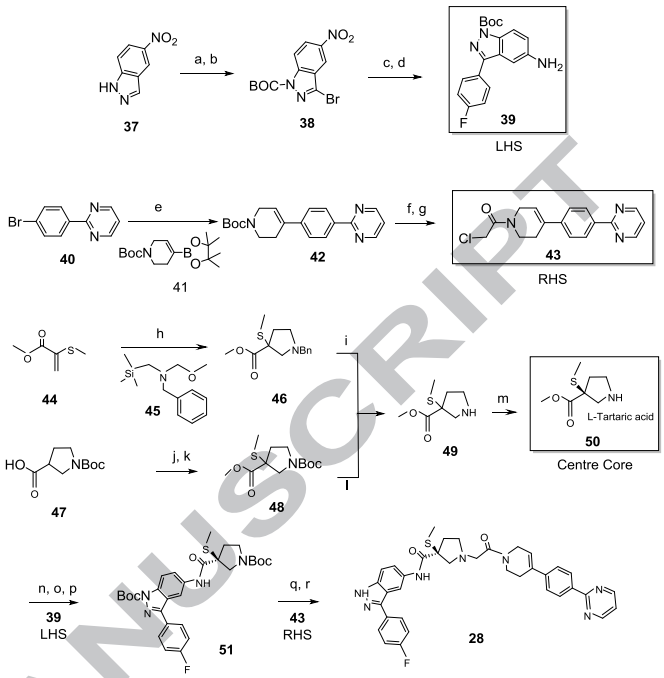

Scheme 1. Synthesis of ERK inhibitor **28**. Reagents and conditions: (a) 1) Br_2, MeOH, 88%; (b) $(Boc)_2O$, DMF, 100%; (c) *p*-flouorphenyl boronic acid, $PdCl_2$(dppf), K_3PO_4, Dioxane/H_2O, 80%; (d) H_2, Pd/C, 100%; (e) **41**, $PdCl_2$(dppf), K_3PO_4, Dioxane/H_2O, 73%; (f) 4.0 N HCl/Dioxane; (g) Chloro acetyl chloride, DIPEA, 80% (two steps); (h) Mont-K-10, 10% w/w, rt, CH_2Cl_2, 3 d, 60%; (i) 1-chloroethyl chloroformate, proton sponge, CH_2Cl_2, 86%; (j) CH_2N_2, MeOH, 100%; (k) LDA, $(SMe)_2$, THF, -78°C, 60%; (l) TFA, CH_2Cl_2, 90%; (m) L-tartaric acid, MeOH, 78%; (n) $(Boc)_2O$, DMF, 100%; (o) *aq*. LiOH (2.0M), THF/MeOH, 100%; (p) **39,** HATU, DIPEA, DMF, 60%; (q) TFA, CH_2Cl_2, 100%; (r) **43**, Et_3N, CH_2Cl_2, 60-80%.

In summary, systematic exploration of sterics and composition at the C-3 position of the pyrrolidine of lead compound **5** led to the discovery of the novel 3(*S*)-thiomethyl pyrrolidine centre core, intermediate **50**, which was shown to play a critical role in achieving vastly improved PK and proved critical in identifying orally bioavailable ERK inhibitors such as compound **28**. In addition, single X-ray crystallography of 3(*S*)-thiomethyl pyrrolidine **27** bound to ERK illustrated a unique binding mode for this class of inhibitors. Finally, the 3(*S*)-thiomethyl pyrrolidine core identified in the work described herein, prominently featured in the development of clinical candidate[18] ERK Inhibitor MK-8353, work which will be reported in due course.

Acknowledgments

We thank Drs. John Piwinski, Cathy Strader, Cecil Pickett at Merck & Co., Inc., Kenilworth, NJ USA for their support and encouragement.

References and notes

1. Yoon, S.; Seger, R. *Growth Factors*, **2006**, *24*, 21.
2. (a) Dhillon, A. S.; Hagan, S.; Rath, O.; Kolch, W. *Oncogene* 2007, 26, 3279 (b) Hanahan, D.; Weinberg, R. A. *Cell*, **2011**, *144*, 646−674.
3. (a) Biomed Valley Discoveries, BVD-523. https://biomed-valley.com/portfolio/bvd-523.
4. Blake, J. F.; Burkard, M.; Chan, J.; Chen, H.; Chou, K. J.; Diaz, D.; Dudley, D. A.; Gaudino, J. J.; Gould, S. E.; Grina, J.;

Hunsaker, T.; Liu, L.; Martinson, M.; Moreno, D.; Mueller, L.; Orr, C.; Pacheco, P.; Qin, A.; Rasor, K.; Ren, L.; Robarge, K.; Shahidi-Latham, S.; Stults, J.; Sullivan, F.; Wang, W.; Yin, J.; Zhou, A.; Belvin, M.; Merchant, M.; Moffat, J.; Schwarz, J. B. *Exp. Rev. of Clin. Immunol*. **2016**, *12*(7), 763.

5. Bagdanoff, J. T.; Jain, R.; Han, W.; Zhu, S.; Madiera, A.-M.; Lee, P. S.; Ma, X.; Poon, D. *Bioorg. Med. Chem. Lett*. **2015**, *25*, 3788
6. Ward, R. A.; Colclough, N.; Challinor, M.; Debreczeni, J. E.; Eckersley, K.; Fairley, G.; Feron, L.; Flemington, V.; Graham, C. R.; Greenwood, R.; Hopcroft, P.; Howard, T. D.; James, M.; Jones, C. D.; Jones, C. R.; Renshaw, J.; Roberts, K.; Snow, L.; Tonge, M.; Yeung, K. *J. Med. Chem*. **2015**, *58*, 4790.
7. Samatar, A. A.; Poulikakos, P.I. *Nature Rev*. **2014**, *13*, 928
8. Wood, K, Luke, J. J. *Curr. Oncol. Rep*., **2016**, *18*, 1
9. Morris, E. J.; Jha, S.; Restaino, C. R.; Dayananth, P.; Zhu, H.; Cooper, A.; Carr, D.; Deng, Y.; Jin, W.; Black, S.; Long, B.; Liu, J.; Dinunzio, E.; Windsor, W.; Zhang, R.; Zhao, S.; Angagaw, M. H.; Pinheiro, E. M.; Desai, J.; Xiao, L.; Shipps, G.; Hruza, A.; Wang, J.; Kelly, J.; Paliwal, S.; Gao, X.; Babu, B. S.; Zhu, L.; Daublain, P.; Zhang, L.; Lutterbach, B. A.; Pelletier, M. R.; Philippar, U.; Siliphaivanh, P.; Witter, D.; Kirschmeier, P.; Bishop, W. R.; Hicklin, D.; Gilliland, D. G.; Jayaraman, L.; Zawel, L.; Fawell, S.; Samatar, A. A. *Cancer Discovery*, **2013**, *3*, 742.
10. (a) Deng, Y.; Shipps Jr, G. W.; Cooper, A. B., English, J. M.; Annis, D. A.; Carr, D.; Nan, Y.; Wang, T.; Zhu, H.Y.; Chuang, C-C.; Dayananth, P.; Hruza, A. W.; Xiao, Li.; Jin, W.; Kirschmeier, P.; Windsor, W. T.; Samatar, A.A. *J. Med. Chem.* **2014,** *57*, 8817 (b) Zhu, H. Y.; Desai, J.; Deng, Y.; Cooper, A. B.; Wang, J.; Shipps, J.; Samatar, A.; Carr, D.; Windsor, W. *Bioorg. Med. Chem. Lett*. **2015**, *25*, 1627
11. Oxidation of (*S*)-3-(methylthio)pyrrolidine-3-carboxylate **50** with *m*CPBA afforded the sulfone intermediate for the synthesis of compound **29**
12. Crystallization of methyl 3-(methylthio)pyrrolidine-3-carboxylate **49** with D-tartaric acid gave the 3(*R*)-thiomethyl pyrrolidine core for the synthesis of compound **32**.
13. (a) Matthews, B. W. *Acc. Chem. Res*. **1988**, *21*, 333 (b) Lipscomb, W. N., Strater, N. *Chem. Rev*. **1996**, *96*, 2375.
14. The binding conformation of compound **27** in ERK2 was taken as a template to mode compound **28**. The change from pipirazine to dihydro-pyridine was made using Maestro (Schrodinger). The structure of the ERK2/**28** complex was further minimized using Macromodel (Schrodinger). Small-Molecule Drug Discovery Suite 2017 , Schrödinger, LLC, New York, NY, 2018.
15. Boga, S. B.; Alhassan, A. B.; Cooper, A. B. Shih, N-Y.; Doll, R. J. *Tetrahedron Lett.*, **2009**, *50*,5315
16. methyl (*S*)-3-(methylthio)pyrrolidine-3-carboxylate **50**:^{1}H NMR (599 MHz, DMSO-d_6): δ 3.98 (s, 1H), 3.69 (s, 2H), 3.53 (d, J = 12.4 Hz, 1H), 3.23 – 3.10 (m, 2H), 2.41 (dt, J = 13.7, 8.2 Hz, 1H), 2.02 – 1.94 (m, 1H). ^{13}C NMR (151 MHz, DMSO-d_6): δ 173.81, 170.95, 71.40, 55.39, 52.45, 52.25, 44.41, 33.67, 12.95.
17. (*S*)-N-(3-(4-fluorophenyl)-1H-indazol-5-yl)-3-(methylthio)-1-(2-oxo-2-(4-(4-(pyrimidin-2-yl)phenyl)-3,6-dihydropyridin-1(2H)-yl)ethyl)pyrrolidine-3-carboxamide **28**: ^{1}H NMR (599 MHz, DMSO-d_6): δ 13.21 (s, 1H), 10.61 (s, 1H), 10.20 – 9.89 (m, 1H), 8.88 (d, J = 4.6 Hz, 2H), 8.42 – 8.29 (m, 3H), 7.93 (m, 3H), 7.69 (dd, J = 8.9, 1.7 Hz, 1H), 7.64 – 7.54 (m, 3H), 7.41 (t, J = 4.7 Hz, 1H), 7.36 (m, 3H), 6.34 (m, 1H), 4.57 (m, 3H), 4.28 – 4.17 (m, 2H), 4.12 (d, , 1H), 3.98 (m, 1H), 3.91 – 3.78 (m, 1H), 3.76 (m, 1H), 3.67 – 3.25 (m, 3H), 2.97 – 2.52 (m, 4H), 2.44 – 2.30 (m, 1H), 2.14 (s, 3H). ^{13}C NMR (151 MHz, DMSO-d_6): δ 168.16, 163.40, 163.17, 162.83, 162.38, 160.75, 157.50, 141.95, 141.57, 138.77, 136.02, 135.99, 134.25, 133.85, 132.25, 130.15, 128.28, 128.23, 127.67, 124.82, 121.28, 121.18, 120.63, 119.63, 119.45, 115.71, 115.57, 110.88, 110.51, 60.91, 59.96, 56.54, 56.04, 55.81, 54.18, 53.64, 43.51, 41.84, 41.26, 33.94, 33.18, 32.71, 26.40, 25.84, 12.88, 12.81.
18. Moschos, S. J; Sullivan, R. J; Flaherty, K. T; Hwu, W-J; Ramanathan, R. K; Adjei, A. A; Fong, P. C; Shapira-Frommer, R; Tawbi, H. A; Rubino, J; Rush, T. S III; Zhang, D; Miselis, N. R; Samatar, A. A; Chun, P; Rubin, E. H; Schiller, J; Long, B. J; Dayananth, P; Carr, D; Kirschmeier, P; Bishop, W. R; Deng, Y; Cooper, A; Shipps, G. W; Moreno, B. H; Robert, L; Ribas, A. *JCI insight*. **2018**, 3(*4*), 1.

Graphical Abstract

To create your abstract, type over the instructions in the template box below.

Discovery of 3(*S*)-thiomethyl pyrrolidine ERK inhibitors for oncology

Leave this area blank for abstract info.

Sobhana Babu Bogaa, * Abdul-Basit Alhassan, Alan B. Cooper, Ronald Doll, Neng-Yang Shih, Gerald Shipps,Yongqi Deng, Hugh Zhu, Yang Nan, Robert Sun, Liang Zhu, Jagdish Desai, Mehul Patel, Kiran Muppalla, Xiaolei Gao, James Wang, Xin Yao, Joseph Kelly, Subrahmanyam Gudipati, Sunil Paliwal, Hon-Chung Tsui, Tong Wang, Bradley Sherborne, Li Xiao, Alan Hruza, Alexei Buevich, Li-Kang Zhang, David Hesk, Ahmed A. Samatar, Donna Carr, Brian Long, Stuart Black, Priya Dayananth, William Windsor, Paul Kirschmeier, Robert Bishop

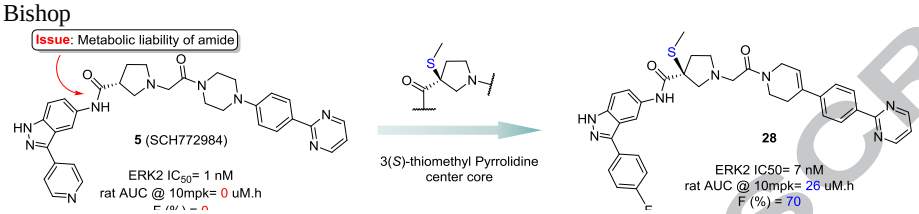

Fonts or abstract dimensions

- Discovery of potent, selective and orally bioavailable ERK inhibitor for oncology
- Synthesis of *tert* 3-(*S*)thiomethyl pyrrolidine based ERK inhibitors
- Improved PK due to sulfur substitution-mitigation of amide bond cleavage